





## Research Article

# Diagnosis of COVID-19 Using a Deep Learning Model in Various Radiology Domains

Yousef Alhwaiti <sup>1</sup>, Muhammad Hameed Siddiqi <sup>1</sup>, Madallah Alruwaili <sup>1</sup>,  
Ibrahim Alrashdi,<sup>1</sup> Saad Alanazi <sup>1</sup>, and Muhammad Hasan Jamal<sup>2</sup>

<sup>1</sup>College of Computer and Information Sciences, Jouf University, Sakaka, Aljouf, 2014, Saudi Arabia

<sup>2</sup>Department of Computer Science, COMSATS University, Islamabad, Lahore Campus, Pakistan

Correspondence should be addressed to Muhammad Hameed Siddiqi; [mhsiddiqi@ju.edu.sa](mailto:mhsiddiqi@ju.edu.sa)

Received 28 April 2021; Accepted 12 August 2021; Published 13 September 2021

Academic Editor: Muhammad Ahmad

Copyright © 2021 Yousef Alhwaiti et al. This is an open access article distributed under the Creative Commons Attribution License, which permits unrestricted use, distribution, and reproduction in any medium, provided the original work is properly cited.

Many countries are severely affected by COVID-19, and various casualties have been reported. Most countries have implemented full and partial lockdowns to control COVID-19. Paramedical employee infections are always a threatening discovery. Front-line paramedical employees might initially be at risk when observing and treating patients, who can contaminate them through respiratory secretions. If proper preventive measures are absent, front-line paramedical workers will be in danger of contamination and can become unintentional carriers to patients admitted in the hospital for other illnesses and treatments. Moreover, every country has limited testing capacity; therefore, a system is required which helps the doctor to directly check and analyze the patients' blood structure. This study proposes a generalized adaptive deep learning model that helps the front-line paramedical employees to easily detect COVID-19 in different radiology domains. In this work, we designed a model using convolutional neural network in order to detect COVID-19 from X-ray, Computed Tomography (CT), and Magnetic Resonance Imaging (MRI) images. The proposed model has 27 layers (input, convolutional, max-pooling, dropout, flatten, dense, and output layers), which has been tested and validated on various radiology domains such as X-ray, CT, and MRI. For experiments, we utilized 70% of the dataset for training and 30% for testing against each dataset. The weighted average accuracies for the proposed model are 94%, 85%, and 86% on X-ray, CT, and MRI, respectively. The experiments show the significance of the model against state-of-the-art works.

## 1. Introduction

The rapid spread of COVID-19 has motivated scientists to quickly develop countermeasures using technologies such as cognitive computing, deep learning, artificial intelligence, machine intelligence, cloud-based collaboration, and wireless communication [1].

Cognitive computing simulates human thought processes and is extensively used in fields such as finance and investment, healthcare and veterinary medicine, travel, and mobile systems [2–4]. The Internet of things (IoT) is implemented on interconnected electronic devices with unique identifiers (UIDs), such as computers, smartphones, coffeemakers, washing machines, and wearable devices

[5, 6]. The IoT, along with cloud computing, Artificial Intelligence (AI), Machine Learning (ML), and deep learning, could be a powerful tool to combat COVID-19 [7, 8], and 4<sup>th</sup> generation (4G) and 5<sup>th</sup> generation (5G) wireless communication technologies have the potential to revolutionize many sectors, including healthcare [9–11]. China has already used 5G technology to fight the COVID-19 pandemic by monitoring patients, collecting and analyzing data, and tracking viruses [1].

Most developing countries utilize wireless technologies, laboratory-based trails, and radiological investigations in order to recognize and diagnose COVID-19 [12]. A standard method is real-time reverse transcription polymerase chain reaction (qRT-PCR), but false-negative results can occur due

to asymptomatic patients, and mistakes may also affect its role in identifying COVID-19 [13, 14]. In the early stages, imaging technologies such as CT scan, MRI, and X-rays might play a vital role in detecting COVID-19 patients [15–17].

Radiology-based chest scanning has been employed to investigate pneumonia [18]. An artificial intelligence- (AI-) based tool was developed [19] to automatically detect, quantify, and monitor COVID-19 and to differentiate affected and normal patients. A deep learning-based approach [20] was developed to automatically segment the entire lung with infection sites under a chest CT. Similarly, an early screening system based on deep learning can discriminate influenza (viral pneumonia) from vigorous cases and COVID-19 [21]. A deep learning-based approach can extract graphical features from CT images of COVID-19 [22]. These features deliver prior medical analysis pathogenic testing and have been claimed to save crucial time for disease investigation. However, most consider just one radiology domain, such as X-ray or CT.

This work builds a deep learning approach in order to notice COVID-19 from various radiological input images such as X-ray, CT, and MRI. The model is a convolutional neural network (CNN) whose 27 layers include input, convolutional, max-pooling, dropout, flatten, dense, and output. The input layer accepts input grayscale images of size  $128 \times 128$  and uses 64 filters of size  $3 \times 3$ . A ReLU activation function is employed in the input layer and all hidden layers. Following the max-pooling layer is a dropout layer to avoid overfitting. This drops out different neurons in the hidden layer. The percentage of neurons to drop should be specified when using the dropout function. We drop 30%. Next are two convolutional layers, both with 128 filters of size  $3 \times 3$ , then a  $2 \times 2$  max-pooling layer, and a dropout layer to drop 30% of neurons. We add three convolutional layers with 256 filters, each with size  $3 \times 3$ , followed by a max-pooling layer with the same parameters as the previous pooling layer. We also drop 30% of the output neurons. We continue increasing filters in more layers, adding three convolutional layers with 512 filters in each layer, with the same filter size as previous layers. A max-pooling layer follows this stack of layers, and 30% of the neurons are dropped. Two stacks, the same as previous layers, are added using the same parameters.

The rest of the paper is organized as follows. Section 2 summarizes state-of-the-art work in various radiology domains. Section 3 presents the proposed methodology. The datasets used in this research are described in Section 4. The experimental environment for the proposed approach is presented in Section 5, and the results are discussed in Section 6. Section 7 discusses conclusions and directions of future work.

## 2. Related Works

Various radiology techniques (e.g., X-ray, CT, and MRI) have been utilized as imaging modalities in the diagnosis of COVID-19, and research has proposed the identification of COVID-19 against different radiology methods, with various limitations.

An early-stage screening model [23] could differentiate COVID-19 patients from normal humans by employing deep learning techniques under pulmonary CT images, with 86.7% accuracy against 618 CT samples. However, the segmentation model employed before feeding it to the learning model could lose some important features and cause misclassification, and only limited radiology images were employed in experiments. An automatic deep CNN system [18] was based on pretrained models under chest X-ray images. This heuristic model utilized limited X-ray images in a controlled domain.

An integrated technique based on an artificial neural network and convolutional CapsNet [24] was developed to identify COVID-19 against chest X-ray images with pill networks. The performance was assessed with binary and multiclass classifications such as infected, normal, and pneumonia, indicating a 97% recognition rate on binary classification and 84% on multiclass classification. There was no rule to find the structure of the artificial neural network, which had no specific scheme to define the structure of neurons, which could be achieved by experience or trial-and-error [25]. When training of the neural network was completed, the network was reduced to a specific value of error on image samples; hence, it provided no optimum outcomes [25].

Some recent systems [18, 26–28] have utilized deep learning and artificial intelligence to identify COVID-19, but only on X-ray images. Similarly, a commercial platform was used to classify infected patients and normal humans [29], with limited contribution from the authors, who utilized only X-rays in experiments. Deep learning and CNN were used to classify positive patients with coronavirus and healthy patients [30]. A very small dataset of X-ray images was used, which might not be applicable in naturalistic domains.

An automated method [31] was proposed to detect COVID-19-positive patients from normal humans, employing a deep learning-based network coupled with gradient-weighted class activation mapping (Grad-CAM) for feature extraction under CT scan images. However, Grad-CAM-based methods require modification of the network architecture, which could degrade accuracy; computational Grad-CAM is expensive [32]; and a non-standard dataset was utilized. A deep CNN, called decompose, transfer, and compose (DeTraC), was used with principal component analysis (PCA) as a feature dimension reduction method to identify coronavirus against chest X-ray images [33]. However, PCA is problematic in the precise assessment of the covariance matrix [34]. Moreover, even modest invariance might not be taken by PCA unless the training data openly deliver this evidence [35]. A deep learning-based system to identify COVID-19 from normal humans had a recognition rate of up to 100% [36], which is not realistic. Only one radiology (X-ray) image was utilized. Similarly, a system was proposed to classify infected, normal, and pneumonia cases with significant accuracy [37], and a deep CNN-based system was proposed to identify patients with coronavirus and normal humans [38]. However, both systems utilized limited X-ray images and used one radiology images.

We develop a deep learning model to accurately categorize the infected patients with COVID-19 and normal humans. The model employs radiology input images such as X-ray, CT, and MRI, through which we can prove the robustness of the model, which is based on 27 layers of a CNN, including input, convolutional, max-pooling, dropout, flatten, dense, and output layers, and shows significant performance on various radiology images such as X-ray, CT scan, and MRI, compared to state-of-the-art methods.

### 3. Materials and Methods

We describe the proposed deep learning-based approach, whose flowchart against X-ray images is shown in Figure 1.

The model is based on a Convolutional Neural Network (CNN) with 27 layers. The input layer accepts a grayscale image of size  $128 \times 128$  and uses 64 filters of size  $3 \times 3$ . A rectified linear unit (ReLU) activation function is used in the input layer and all hidden layers, where ReLU is defined by the relation  $R(z) = \max(0, z)$ , as shown in Figure 2.

The ReLU activation function omits negative pixels in the input image. The second layer is a convolutional layer that has 64 filters of size  $3 \times 3$ . Next is a max-pooling layer that takes the maximum value for each patch of the feature map, with pool size and stride both  $2 \times 2$ .

Next is a dropout layer to avoid overfitting by dropping out different neurons in hidden layers. We drop 30% of the neurons to reduce overfitting. The dropout technique is shown in Figure 3.

The output of the previous layer is flattened to convert a matrix to a single layer. For instance, an output shape of (1, 128, 18) is flattened to (1, 16384). Then, two dense layers with 4096 units each are added. An ReLU activation function is used in both layers. The last layer is the output layer with two neurons, which is the number of classes (COVID-19 positive and COVID-19 negative). A soft-max activation function normalizes the input vector from the previous layer of real numbers to a probability distribution

$$\sigma(Z) \frac{e^{z_i}}{\sum_{j=1}^K e^{z_j}}, \quad \text{for } i = 1, \dots, K \text{ and } Z = (z_1, \dots, z_k) \in R^K. \quad (1)$$

The proposed approach is described in Figure 4.

### 4. Datasets Used

We utilized the following datasets to show the efficacy of the developed approach.

**4.1. X-Ray Image Dataset.** We utilized a radiology dataset with 270 X-ray images from males and females of age 20–55 years, collected from various open sources (used to diagnose coronavirus). During implementation, we regularly updated the dataset to incorporate the latest complex chest X-ray images. The dataset was thoroughly checked by medical experts (physicians). We did not provide metadata for patients. Images were converted to a vector with dimensions  $1 \times 6400$  by decreasing the dimension of every input image to

$80 \times 80$ . To avoid imbalance, we utilized 135 normal patients' images and 135 COVID-19-positive images. The dataset was collected over a period of 3 months (June to August 2020).

**4.2. Computed Tomography (CT) Scan Image Dataset.** The CT image dataset contained 270 chest CT images. The dataset was built from open sources commonly used to diagnose COVID-19. The dataset incorporated new complex CT scan images that were systematically checked by doctors. The images were from males and females of age 35 to 55 years. For experiments, images in this dataset were transformed to a vector with dimensions  $1 \times 6400$  by decreasing the dimension of every input image to  $80 \times 80$ . To avoid imbalance, we utilized images of 135 normal patients and 135 images from COVID-19-positive patients. The dataset was collected over 3 months (June to August 2020).

**4.3. Magnetic Resonance Imaging (MRI) Image Dataset.** Another type of radiology dataset was of MRI scans, which generate two types of images. T1-weighted images highlight (brighten) lipids and fats by a radio-frequency pulse sequence, and T2-weighted images highlight also water. So, the timing of the radiofrequency pulse sequence highlights the target tissues. We included 270 MRI images of males and females of age 35 to 60 years. These were confirmed cases of COVID-19. We added controls with approximately similar ages and genders but without COVID-19. All images were converted to a vector of dimension  $1 \times 6400$  by decreasing the dimension of every input image to  $80 \times 80$ . To avoid imbalance, we utilized 135 images of normal patients and 135 COVID-19-positive images. The dataset was collected over 3 months (June to August 2020).

## 5. Experimental Setup

We performed many experiments to show the significance of the proposed model against each dataset; these were divided into 70% for training and 30% for testing for all tested algorithms. The same model architecture was used for each dataset, with different hyperparameters.

All experiments were performed using Python, TensorFlow, and Google Colab (for training) on an Intel Pentium Core i7-6700 (3.4 GHz) with 16 GB RAM. Experiments are described as follows:

- (i) The first experiment assessed the proposed model against chest X-ray, CT scan, and MRI datasets through an average cross-validation scheme.
- (ii) The second experiment included a set of sub-experiments performed under the absence of the developed approach against all three datasets. We utilized logistic regression, support vector machine, random forest, k-nearest neighbor, artificial neural network, Naive Bayes, decision tree, passive aggressive classifier, multilayer perceptron, and extra tree classifiers.
- (iii) The third experiment compared the proposed technique to the state of the art.

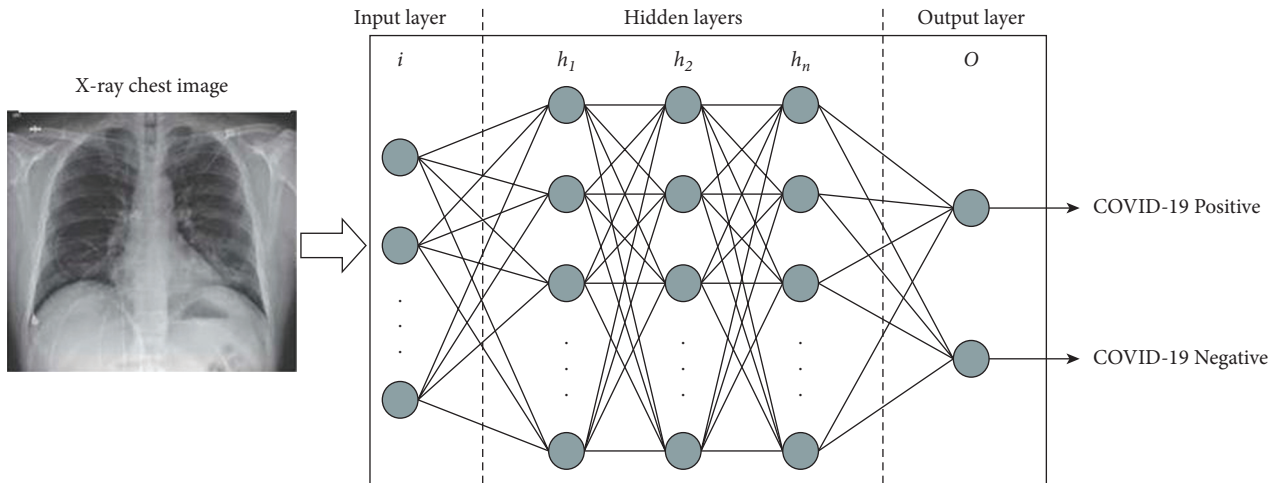


FIGURE 1: Flow diagram of the proposed approach against X-ray images.

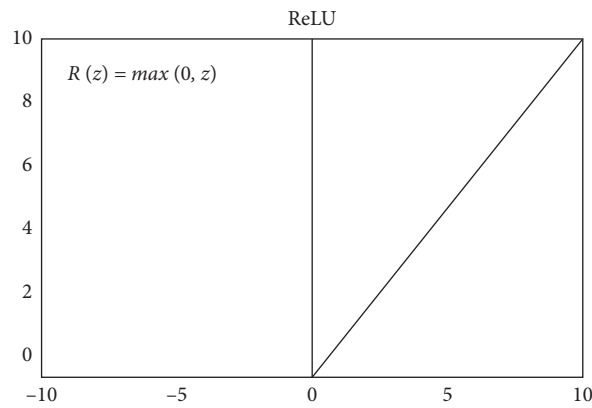


FIGURE 2: ReLU activation function [39].

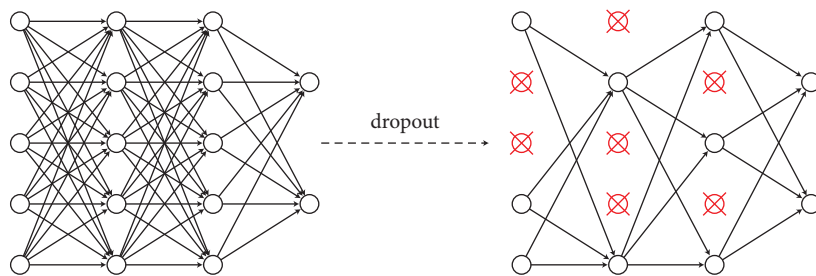


FIGURE 3: Dropout technique [40].

## 6. Results and Discussion

6.1. *First Experiment.* The results of the first experiment are shown in Table 1.

As can be seen from Table 1, the model got significant accuracy among state of the art. It trained in different datasets with different hyperparameters using same structure of the model. That indicates that the structure of the model is significant. Also, the model was compared with different machine

learning algorithms to show the difference in accuracy between deep learning and regular machine learning algorithms.

6.2. *Second Experiment.* The results of the second experiment are presented in Tables 2–11.

We observe from Tables 2–11 that all of the existing classifiers did not achieve better accuracy against the three datasets. This is because most of the medical images are

Layer (type)	Output Shape	Param #			
conv2d (Conv2D)	(None, 128, 128, 64)	640	conv2d_7 (Conv2D)	(None, 16, 16, 512)	1180160
conv2d_1 (Conv2D)	(None, 128, 128, 64)	36928	conv2d_8 (Conv2D)	(None, 16, 16, 512)	2359808
max_pooling2d (MaxPooling2D)	(None, 64, 64, 64)	0	conv2d_9 (Conv2D)	(None, 16, 16, 512)	2359808
dropout (Dropout)	(None, 64, 64, 64)	0	max_pooling2d_3 (MaxPooling2)	(None, 8, 8, 512)	0
conv2d_2 (Conv2D)	(None, 64, 64, 128)	73856	dropout_3 (Dropout)	(None, 8, 8, 512)	0
conv2d_3 (Conv2D)	(None, 64, 64, 128)	147584	conv2d_10 (Conv2D)	(None, 8, 8, 512)	2359808
max_pooling2d_1 (MaxPooling2)	(None, 32, 32, 128)	0	conv2d_11 (Conv2D)	(None, 8, 8, 512)	2359808
dropout_1 (Dropout)	(None, 32, 32, 128)	0	conv2d_12 (Conv2D)	(None, 8, 8, 512)	2359808
conv2d_4 (Conv2D)	(None, 32, 32, 256)	295168	max_pooling2d_4 (MaxPooling2)	(None, 4, 4, 512)	0
conv2d_5 (Conv2D)	(None, 32, 32, 256)	590080	dropout_4 (Dropout)	(None, 4, 4, 512)	0
conv2d_6 (Conv2D)	(None, 32, 32, 256)	590080	flatten (Flatten)	(None, 8192)	0
max_pooling2d_2 (MaxPooling2)	(None, 16, 16, 256)	0	dense (Dense)	(None, 4096)	33558528
dropout_2 (Dropout)	(None, 16, 16, 256)	0	dense_1 (Dense)	(None, 4096)	16781312
			dense_2 (Dense)	(None, 2)	8194
			=====		
			Total params: 65,061,570		
			Trainable params: 65,061,570		
			Non-trainable params: 0		

(a)

(b)

FIGURE 4: (a), (b) The workflow of the proposed model.

TABLE 1: Recognition rates of the proposed approach against X-ray, CT, and MRI datasets.

Datasets	Recognition rates	
X-ray	Classified	94%
	Misclassified	6%
CT scan	Classified	85%
	Misclassified	15%
MRI	Classified	86%
	Misclassified	16%

TABLE 2: Recognition rates of logistic regression (under the absence of the proposed approach) against X-ray, CT, and MRI datasets.

Datasets	Recognition rates	
X-ray	Classified	73%
	Misclassified	27%
CT scan	Classified	65%
	Misclassified	35%
MRI	Classified	74%
	Misclassified	26%

sensitive to noise and other environmental factors. The proposed approach can achieve significant accuracy under the presence of noise and other environmental factors, as shown in Table 1.

**6.3. Third Experiment.** The recognition rates of the proposed model and other models are shown in Tables 12–14, which present that the proposed model achieved higher accuracy on all three datasets.

As illustrated in Tables 12–14, the proposed approach achieved higher accuracy than other recent works under all the three radiology datasets.

**6.4. Discussion.** COVID-19 has affected millions of people around the world. The early detection of COVID-19 could help in stopping the spread. One of the most effective detections is screening the infected patients. Deep learning plays an affective role in this detection, and it is more



TABLE 3: Recognition rates of support vector machine (under the absence of the proposed approach) against X-ray, CT, and MRI datasets.

Datasets	Recognition rates	
X-ray	Classified	75%
	Misclassified	25%
CT scan	Classified	51%
	Misclassified	49%
MRI	Classified	78%
	Misclassified	22%

TABLE 4: Recognition rates of random forest (under the absence of the proposed approach) against X-ray, CT, and MRI datasets.

Datasets	Recognition rates	
X-ray	Classified	79%
	Misclassified	21%
CT scan	Classified	74%
	Misclassified	26%
MRI	Classified	77%
	Misclassified	23%

TABLE 5: Recognition rates of k-nearest neighbor (under the absence of the proposed approach) against X-ray, CT, and MRI datasets.

Datasets	Recognition rates	
X-ray	Classified	79%
	Misclassified	21%
CT scan	Classified	69%
	Misclassified	31%
MRI	Classified	81%
	Misclassified	19%

TABLE 6: Recognition rates of support vector machine (under the absence of the proposed approach) against X-ray, CT, and MRI datasets.

Datasets	Recognition rates	
X-ray	Classified	72%
	Misclassified	28%
CT scan	Classified	66%
	Misclassified	34%
MRI	Classified	79%
	Misclassified	21%

TABLE 7: Recognition rates of Naïve Bayes (under the absence of the proposed approach) against X-ray, CT, and MRI datasets.

Datasets	Recognition rates	
X-ray	Classified	80%
	Misclassified	20%
CT scan	Classified	58%
	Misclassified	42%
MRI	Classified	77%
	Misclassified	23%

TABLE 8: Recognition rates of decision tree (under the absence of the proposed approach) against X-ray, CT, and MRI datasets.

Datasets	Recognition rates	
X-ray	Classified	72%
	Misclassified	28%
CT scan	Classified	65%
	Misclassified	35%
MRI	Classified	77%
	Misclassified	23%

TABLE 9: Recognition rates of passive aggressive classifier (under the absence of the proposed approach) against X-ray, CT, and MRI datasets.

Datasets	Recognition rates	
X-ray	Classified	65%
	Misclassified	35%
CT scan	Classified	71%
	Misclassified	29%
MRI	Classified	70%
	Misclassified	30%

TABLE 10: Recognition rates of multilayer perceptron (under the absence of the proposed approach) against X-ray, CT, and MRI datasets.

Datasets	Recognition rates	
X-ray	Classified	60%
	Misclassified	40%
CT scan	Classified	66%
	Misclassified	34%
MRI	Classified	47%
	Misclassified	53%

TABLE 11: Recognition rates of extra tree classifier (under the absence of the proposed approach) against X-ray, CT, and MRI datasets.

Datasets	Recognition rates	
X-ray	Classified	81%
	Misclassified	19%
CT scan	Classified	79%
	Misclassified	21%
MRI	Classified	79%
	Misclassified	21%

TABLE 12: The comparison of the proposed approach along with the state-of-the-art methods on the X-ray dataset (unit: %).

State of the art	Weighted average recognition rates	Standard deviation
[28]	89.6	$\pm 2.9$
[30]	83.5	$\pm 3.7$
[41]	80.3	$\pm 2.6$
[42]	85.4	$\pm 1.2$
[43]	79.8	$\pm 3.8$
[44]	89.3	$\pm 2.3$
[45]	91.5	$\pm 1.9$
[46]	90.5	$\pm 2.7$
Proposed model	94.0	$\pm 3.5$

TABLE 13: The comparison of the proposed approach along with the state-of-the-art methods on the CT scan dataset (unit: %).

State of the art	Weighted average recognition rates	Standard deviation
[28]	82.3	$\pm 1.7$
[47]	75.2	$\pm 1.9$
[48]	84.7	$\pm 2.1$
[49]	82.4	$\pm 2.5$
[50]	83.4	$\pm 1.2$
[51]	79.2	$\pm 3.6$
Proposed model	85.0	$\pm 3.5$

accurate. There are many studies implemented in to detect COVID-19 using deep learning. In this research, we have used a deep learning neural network (convolutional neural network) to detect COVID-19 from different radiologists. Our model results are comparable to the state of the art

because we have built a robust model. What made our model a comparable result is that we build the model using different layers (27 layers), adjusting hyperparameters, using effective percentage in dropout, size of the filters in convolutional and pool layers, and using a suitable way in preprocessing. These

TABLE 14: The comparison of the proposed approach along with the state-of-the-art methods on the MRI dataset (unit: %).

State of the art	Weighted average recognition rates	Standard deviation
Logistic regression	74.0	$\pm 3.1$
Support vector machine	78.0	$\pm 1.8$
Random forest	77.0	$\pm 2.4$
k-nearest neighbor	81.0	$\pm 1.1$
Artificial neural network	79.0	$\pm 3.7$
Naïve Bayes	71.0	$\pm 5.2$
Decision tree	77.0	$\pm 2.6$
Passive aggressive classifier	70.0	$\pm 4.6$
Multilayer perceptron	47.0	$\pm 6.1$
Extra tree classifier	79.0	$\pm 4.4$
Proposed model	86.0	$\pm 3.5$

layers include input, convolutional, max-pooling, dropout, flatten, dense, and output. The input layer accepts input grayscale images of size  $128 \times 128$  and uses 64 filters of size  $3 \times 3$ . An ReLU activation function is used in the input layer and all hidden layers. Following the max-pooling layer is a dropout layer to avoid overfitting. This drops out different neurons in the hidden layer. The percentage of neurons to drop should be specified when using the dropout function. We drop 30%. Next are two convolutional layers, both with 128 filters of size  $3 \times 3$ , then a  $2 \times 2$  max-pooling layer, and a dropout layer to drop 30% of neurons. We add three convolutional layers with 256 filters, each with size  $3 \times 3$ , and then a max-pooling layer with the same parameters as the previous pooling layer. We also drop 30% of the output neurons. We continue increasing filters in more layers, adding three convolutional layers with 512 filters in each layer, with the same filter size as previous layers. A max-pooling layer follows this stack of layers, and 30% of the neurons are dropped. Two stacks, the same as previous layers, are added using the same parameters. Moreover, the model got significant accuracy among the state of the art. It trained in different datasets with different hyperparameters using same structure of the model. That indicates that the structure of the model is significant. Also, the model was compared with different machine learning techniques to show the difference in accuracy between deep learning and regular machine learning algorithms.

## 7. Conclusions

We developed a model to efficiently detect COVID-19 from different radiology techniques and showed its robustness on X-ray, CT, and MRI datasets. We used a CNN to build the deep learning model, which gives adequate image classification. To show the performance of the proposed model, many experiments were performed against each dataset. In the first experiment, we built a model using a CNN with different layers and trained it on the first dataset, and the same model constructor was used to train the other datasets. For each dataset, we adjusted the hyperparameters for the model to get a robust model. In the second experiment, we utilized different machine learning algorithms on each dataset (in the absence of the proposed model). This demonstrated the importance and significance of the proposed model. Regardless of the lack of instances in a dataset, our model had

high classification accuracy for COVID-19. Finally, the classification rates of our technique were compared to those of the previous work, and the developed approach presented the best performance on various radiology datasets.

The proposed system was tested and validated in a controlled environment. In future research, we will deploy the system in real healthcare systems in which COVID-19 is easily detected from real images.

## Data Availability

The data utilized in order to support the discoveries of this work are described in the paper and will be offered by the corresponding author upon request.

## Conflicts of Interest

The authors declare no conflicts of interest regarding the present study.

## Acknowledgments

This study was supported by Jouf University, Sakaka, Aljouf, Kingdom of Saudi Arabia, under grant no. DSR2020-06-3675.

## References

- [1] V. Chamola, V. Hassija, V. Gupta, and M. Guizani, "Comprehensive review of the COVID-19 pandemic and the role of IoT, drones, AI, blockchain, and 5G in managing its impact," *IEEE Access*, vol. 8, pp. 90225–90265, 2020.
- [2] K. Lin, C. Li, D. Tian, A. Ghoneim, M. S. Hossain, and S. U. Amin, "Artificial-intelligence-based data analytics for cognitive communication in heterogeneous wireless networks," *IEEE Wireless Communications*, vol. 26, no. 3, pp. 83–89, 2019.
- [3] Y. Zhang, Y. Qian, D. Wu, M. S. Hossain, and A. Ghoneim, M. Chen, "Emotion-aware multimedia systems security," *IEEE Transactions on Multimedia*, vol. 21, no. 3, pp. 617–624, 2018.
- [4] M. S. Hossain and G. Muhammad, "An audio-visual emotion recognition system using deep learning fusion for a cognitive wireless framework," *IEEE Wireless Communications*, vol. 26, no. 3, pp. 62–68, 2019.
- [5] Y. Zhang, X. Ma, J. Zhang, M. S. Hossain, G. Muhammad, and S. U. Amin, "Edge intelligence in the cognitive internet of



- things: improving sensitivity and interactivity,” *IEEE Network*, vol. 33, no. 3, pp. 58–64, 2019.
- [6] M. A. Rahman, M. M. Rashid, M. S. Hossain, E. Hassanain, M. F. Alhamid, and M. Guizani, “Blockchain and IoT-based cognitive edge framework for sharing economy services in a smart city,” *IEEE Access*, vol. 7, pp. 18611–18621, 2019.
  - [7] S. A. Alanazi, M. M. Kamruzzaman, M. Alruwaili, N. Alshammari, S. A. Alqahtani, and A. Karime, “Measuring and preventing COVID-19 using the SIR model and machine learning in smart health care,” *Journal of Healthcare Engineering*, vol. 2020, Article ID 8857346, 12 pages, 2020.
  - [8] M. M. Kamruzzaman, “Architecture of smart health care system using artificial intelligence,” in *Proceedings of the IEEE International Conference on Multimedia & Expo Workshops*, pp. 1–6, London, UK, July 2020.
  - [9] Y. Zhang, M. S. Hossain, A. Ghoneim, and M. Guizani, “COcME: content-oriented caching on the mobile edge for wireless communications,” *IEEE Wireless Communications*, vol. 26, no. 3, pp. 26–31, 2019.
  - [10] J. Wang, Y. Miao, P. Zhou, M. S. Hossain, and S. M. M. Rahman, “A software defined network routing in wireless multihop network,” *Journal of Network and Computer Applications*, vol. 85, pp. 76–83, 2017.
  - [11] A. Alelaiwi, A. Alghamdi, M. Shorfuzzaman, M. Rawashdeh, M. S. Hossain, and G. Muhammad, “Enhanced engineering education using smart class environment,” *Computers in Human Behavior*, vol. 51, pp. 852–856, 2015.
  - [12] M. Shahzeb, A. Khan, and A. Muhammad, “Detection of coronavirus disease (COVID-19) using radiological examinations,” *Journal of Pure Applied Microbiology*, vol. 14, 2020.
  - [13] H. J. Shi, J. Yu, and C. S. Zheng, “Radiological diagnosis of new coronavirus infected pneumonitis: expert recommendation from the Chinese society of radiology,” *Zhonghua Fang She Xue Za Zhi*, vol. 54, pp. 279–285, 2020.
  - [14] J. F. W. Chan, S. Yuan, K. H. Kok et al., “A familial cluster of pneumonia associated with the 2019 novel coronavirus indicating person-to-person transmission: a study of a family cluster,” *The Lancet*, vol. 395, no. 10223, pp. 514–523, 2020.
  - [15] H. Fu, H. Xu, N. Zhang, H. Xu, and Z. Li, H. Chen, R. Xu, R. Sun et al., “Association between clinical, laboratory and CT characteristics and RT-PCR results in the follow-up of COVID-19 patients,” *MedRxiv*, 2020.
  - [16] General Office of National Health Committee and others, “Office of state administration of traditional Chinese medicine (2020),” *Notice on the Issuance of a Program for the Diagnosis and Treatment of Novel Coronavirus (2019-nCoV) Infected Pneumonia (Trial Fifth Edition)*, 2020.
  - [17] J. P. Kanne, “Chest CT findings in 2019 novel coronavirus (2019-nCoV) infections from Wuhan, China: key points for the radiologist,” *Radiology*, vol. 295, 2020.
  - [18] A. Narin, C. Kaya, and Z. Pamuk, “Automatic detection of coronavirus disease (covid-19) using X-ray images and deep convolutional neural networks,” 2020, <https://arxiv.org/abs/2003.10849>.
  - [19] O. Gozes, M. Frid-Adar, H. Greenspan et al., “Rapid AI development cycle for the coronavirus (covid-19) pandemic: initial results for automated detection & patient monitoring using deep learning CT image analysis,” 2020, <https://arxiv.org/abs/2003.05037>.
  - [20] F. Shan, Y. Gao, J. Wang et al., “Lung infection quantification of covid-19 in CT images with deep learning,” 2020, <https://arxiv.org/abs/2003.04655>.
  - [21] C. Butt, J. Gill, D. Chun, and B. A. Babu, “Deep learning system to screen coronavirus disease 2019 pneumonia,” *Applied Intelligence*, p. 1, 2020.
  - [22] S. Wang, B. Kang, J. Ma, X. Zeng, and M. Xiao, “A deep learning algorithm using CT images to screen for coronavirus disease (COVID-19),” *MedRxiv*, 2020.
  - [23] X. Xu, X. Jiang, C. Ma et al., “Deep learning system to screen coronavirus disease 2019 pneumonia,” 2020, <https://arxiv.org/abs/2002.09334>.
  - [24] S. Toraman, T. B. Alakus, and I. Turkoglu, “Convolutional capsnet: a novel artificial neural network approach to detect COVID-19 disease from X-ray images using capsule networks,” *Chaos, Solitons & Fractals*, vol. 140, pp. 110–122, 2020.
  - [25] M. M. Mijwel, “Artificial neural networks advantages and disadvantages,” 2018, <https://www.linkedin.com/pulse/artificial-neuralnet-works-advantages-disadvantages-maadm-mijwel>.
  - [26] M. K. Pandit and S. A. Banday, “SARS n-CoV2-19 detection from chest X-ray images using deep neural networks,” *International Journal of Pervasive Computing and Communications*, vol. 16, 2020.
  - [27] M. Ilyas, H. Rehman, and A. Nait-Ali, “Detection of COVID-19 from chest X-ray images using artificial intelligence: an early review,” 2020, <https://arxiv.org/abs/2004.05436>.
  - [28] S. H. Kassani, P. H. Kassasni, M. J. Wesolowski, K. A. Schneider, and R. Deters, “Automatic detection of coronavirus disease (COVID-19) in X-ray and CT images: a machine learning-based approach,” 2020, <https://arxiv.org/abs/2004.10641>.
  - [29] A. A. Borkowski, N. A. Viswanadham, L. B. Thomas, R. D. Guzman, L. A. Deland, and S. M. Mastorides, “Using artificial intelligence for COVID-19 chest X-ray diagnosis,” *Medrxiv*, vol. 37, 2020.
  - [30] A. Makris, I. Kontopoulos, and K. Tserpes, “COVID-19 detection from chest X-ray images using deep learning and convolutional neural networks,” in *Proceedings of the 11th Hellenic Conferences on Artificial Intelligence*, pp. 60–66, Athens, Greece, September 2020.
  - [31] M. Rahimzadeh, A. Attar, and S. M. Sakhaei, “A fully automated deep learning-based network for detecting COVID-19 from a new and large lung CT scan dataset,” *MedRxiv*, 2020.
  - [32] R. R. Selvaraju, M. Cogswell, A. Das, R. Vedantam, D. Parikh, and D. Batra, “Grad-cam: visual explanations from deep networks via gradient-based localization,” in *Proceedings of the IEEE International Conferences on Computer Vision*, pp. 618–626, Venice, Italy, October 2017.
  - [33] A. Abbas, M. M. Abdelsamea, and M. M. Gaber, “Classification of COVID-19 in chest X-ray images using DeTraC deep convolutional neural network,” *Applied Intelligence*, 2020.
  - [34] P. J. Phillips, P. J. Flynn, T. Scruggs et al., “Overview of the face recognition grand challenge,” in *Proceedings of the IEEE Computer Society Conference on Computer Vision and Pattern Recognition (CVPR’05)*, pp. 947–954, San Diego, CA, USA, June 2005.
  - [35] C. Li, Y. Diao, H. Ma, and Y. Li, “A statistical PCA method for face recognition,” in *Proceedings of the 2nd International Symposium on Intelligent Information Technology Application*, pp. 376–380, Shanghai, China, December 2008.
  - [36] J. Civit-Masot, F. Luna-Perejón, M. Domínguez Morales, and A. Civit, “Deep learning system for COVID-19 diagnosis aid using X-ray pulmonary images,” *Applied Sciences*, vol. 10, no. 13, p. 4640, 2020.
  - [37] T. Ozturk, M. Talo, E. A. Yildirim, U. B. Baloglu, O. Yildirim, and U. Rajendra Acharya, “Automated detection of COVID-

- 19 cases using deep neural networks with X-ray images,” *Computers in Biology and Medicine*, vol. 121, Article ID 103792, 2020.
- [38] A. K. Das, S. Ghosh, S. Thunder, R. Dutta, S. Agarwal, and A. Chakrabarti, “Automatic COVID-19 detection from X-ray images using ensemble learning with convolutional neural network,” *Pattern Analysis and Application*, vol. 24, 2020.
- [39] C. Dabakoglu, “Convolutional neural network,” 2020, <https://medium.com/@cdabakoglu/what-is-convolutional-neural-networkcnn-with-keras-cab447ad204c>.
- [40] J. Ricco, “Max-pooling/pooling,” 2020, [https://computer-science-wiki.org/index.php/Max-pooling/\\_Pooling](https://computer-science-wiki.org/index.php/Max-pooling/_Pooling).
- [41] R. Jain, M. Gupta, S. Taneja, and D. J. Hemanth, “Deep learning based detection and analysis of COVID-19 on chest X-ray images,” *Applied Intelligence*, pp. 1–11, 2020.
- [42] G. Jain, D. Mittal, D. Thakur, and M. K. Mittal, “A deep learning approach to detect Covid-19 coronavirus with X-ray images,” *Biocybernetics and Biomedical Engineering*, vol. 40, no. 4, pp. 1391–1405, 2020.
- [43] M. Alazab, A. Awajan, A. Mesleh, A. Abraham, V. Jatana, and S. Alhyari, “COVID-19 prediction and detection using deep learning,” *International Journal of Computer Information Systems and Industrial Management Applications*, vol. 12, pp. 168–181, 2020.
- [44] M. M. Rahaman, C. Li, Y. Yao et al., “Identification of COVID-19 samples from chest X-ray images using deep learning: a comparison of transfer learning approaches,” *Journal of X-Ray Science and Technology*, vol. 28, pp. 1–19, 2020.
- [45] B. Sekeroglu and I. Ozsahin, “Detection of COVID-19 from chest X-ray images using convolutional neural networks,” *SLAS Technology: Translating Life Sciences Innovation*, vol. 25, no. 6, pp. 553–565, 2020.
- [46] A. Mangal, S. Kalia, H. Rajgopal, K. Rangarajan, and V. Namboodiri, “CovidAID: COVID-19 detection using chest X-ray,” 2020, <https://arxiv.org/abs/2004.09803>.
- [47] P. Silva, E. Luz, G. Silva et al., “COVID-19 detection in CT images with deep learning: a voting-based scheme and cross-datasets analysis,” *Informatics in Medicine Unlocked*, vol. 20, Article ID 100427, 2020.
- [48] C. Zheng, X. Deng, Q. Fu et al., “Deep learning-based detection for COVID-19 from chest CT using weak label,” *MedRxiv*, 2020.
- [49] H. Alshazly, C. Linse, E. Barth, and T. Martinetz, “Explainable COVID-19 detection using chest CT scans and deep learning,” 2020, <https://arxiv.org/abs/2011.05317>.
- [50] H. J. A. Adams, T. C. Kwee, D. Yakar, M. D. Hope, and R. M. Kwee, “Chest CT imaging signature of coronavirus disease 2019 infection: in pursuit of the scientific evidence,” *Chest*, vol. 158, no. 5, pp. 1885–1895, 2020.
- [51] K. Purohit, A. Kesarwani, D. R. Kisku, and M. Dalui, “Covid-19 detection on chest X-ray and CT scan images using multi-image augmented deep learning model,” *BioRxiv*, 2020.